PREPRINT 10-HZ-INJECTION AT A LASER FOCUS OF TARGETS ACCELERATED INTO A SPRING-HTSC-MAGLEV SYSTEM

E.R. KORESHEVA P.N. Lebedev Physical Institute of RAS Moscow, Russia Email: koreshevaer@lebedev.ru

I.V. ALEKSANDROVA, M.N. AGAPOV, A.A. AKUNETS, A.I. NIKITENKO P.N. Lebedev Physical Institute of RAS Moscow, Russia

Abstract

Cryogenic fuel target (CFT) injection is a critical component of the phased strategy to develop and demonstrate successful target technologies for ICF/IFE applications. This opens a way to implement a uniform laser irradiation of CFTs which are flying in the reaction chamber. The paper goal is the development of basics and concepts for CFT injection at least at a rate of 10 Hz that is characteristic of IFE reactor. For this, a setup based on magnetic levitation (MAGLEV) technologies was created to demonstrate credible solutions in the area of CFTs noncontact transport and their repeatable injection. Herewith, a necessary element is a levitating CFT carrier made from Type-II, high-temperature superconductors (HTSCs). This paper discusses four principal categories: 1) tandem HTSC-carrier configuration (design and materials); 2) construction of a linear permanent magnet guideway (PMG) to maintain a friction-free acceleration of the HTSC-carrier; 3) development of a spring mechanism for driving the HTSC-carrier; 4) development of an optical tracking system to control the HTSC-carrier and injected targets motion. In demo experiments (T = 80 K), a magnetic track (size $360 \times 24 \times 5 \text{ mm}$) had a cross-sectional magnetic induction gradient $\Delta B = 0.33$ T to provide a required stability of the levitation height over the whole acceleration length. The motion of the HTSC-carrier (size 50×4×4 mm, mass 0.55 g weight) containing two surrogate targets (3-mm-glass beads) was recorded, followed by HTSC-carrier mechanical braking and targets injection with a rate of 10 Hz (target nest from foam polymers) and 25 Hz (target nest from full density polymers). A soft electromagnetic option of the HTSC-carrier braking using two ring permanent magnets were also analyzed. Further development of the proposed approach will allow to demonstrate the CFT acceleration, injection and tracking systems, and to obtain new results under conditions of the uniform irradiation of CFTs on existing laser drivers.

1. INTRODUCTION

Fuel supply for high-power laser facilities or inertial fusion energy (IFE) reactor is a key component in the controlled thermonuclear fusion research program. Fuel supply includes: 1) manufacturing of the free standing (un-mounted) CFTs and 2) finished CFTs injection into the reaction chamber at rates as high as 5–10 Hz with a precise CFT` location to achieve their uniform, spherically symmetric irradiation by a laser.

The features of scientific and technological problems associated with the first task are discussed in detail in [1]. The present work is devoted to the second task: CFT delivery by injection both in a single and a repeatable mode with a rate at least of 10 Hz.

At present, in existing inertial confinement fusion (ICF) facilities, laser irradiation is carried out on a CFT, previously fixed at the laser focus using a special suspension (thread, capillary, cone, film, etc.; see, for example, [2]). The presence of a material contact between the suspension and the CFT does not allow the fundamental requirement of ICF to be realized: uniform or spherically symmetric irradiation of CFT. The problem solution lies in the implementation of the CFT delivery by injection.

For this goal, innovative technologies for the creation of a noncontact HTSC-MAGLEV accelerator with a levitating CFT-carrier are intensively developed at the Lebedev Physical Institute (LPI). The studies are based on the phenomenon of quantum levitation of HTSCs in the gradient magnetic fields. The basics and concepts for HTSC-MAGLEV acceleration for ICF/IFE can be found in [3, 4].

To solve the injection problem it is important to clearly distinguish two different options in the research: injection rates for ICF (existing laser facilities) and for IFE (future reactor). Using ICF laser facilities opens up new perspectives and new capabilities in HTSC-MAGLEV application for laser ICF/IFE. It will allow to

integrate the operation of target acceleration, injection and tracking systems, and to enhance the CFT performance during implosion when the laser beams will be focused on the CFT surface in a uniform pattern. For IFE reactor (chamber radius $R_{\rm ch} \sim 6$ m [5]), the CFT with a temperature of $T \sim 18$ K must be accelerated to high injection speeds of 200–400 m/s to withstand the high temperature environment of the reaction chamber (wall temperature is $T_{\rm ch} \sim 1758$ K [5]). According to the Stefan-Boltzmann law $J_0 = \sigma T^4$, the value of the thermal radiation flux density J_0 coming from the hot chamber walls and incident on the CFT surface is proportional to the fourth power of the temperature. Taking this into account, the requirements for the CFT injection rate for the existing ICF laser facilities ($T_{\rm ch} = 300$ K and $R_{\rm ch} = 1-5$ m) can be an order of magnitude lower. The mathematical modeling performed in [6] has confirmed this assumption. For a low initial aspect ratio (A = 3 and A = 5), the direct-drive targets with a 300 μ g-DT mass [7] have a speed range of $v_{\rm inj} = 3.2-17$ m/s, which is significantly lower than for IFE reactor. This makes it possible to start developing a CFT injection system operating at room temperature and to demonstrate key issues for the injection process on existing laser facilities (Table 1). Then, one can integrate the target acceleration, injection and tracking systems into a single system at room temperature $T_{\rm ch}$, and then upgrade it to cryogenic operations and high temperature chamber wall.

TABLE 1. THE REQUIRED INJECTION SPEED OF THE CFT (m/s) FOR ITS ACCURATE PLACEMENT IN THE CENTER OF THE REACTION CHAMBER

R _{ch} (m)	$\alpha = 45^{\circ}$	$\alpha = 30^{\circ}$	$\alpha = 15^{\circ}$	α = 10°	$\alpha = 5^{\circ}$	Note: ICF laser facilities
5.0	7.1	7.6	9.8	12.1	17.0	UFL-2M [8], NIF [9], LMJ [10]
0.9	3.2	3.4	4.5	5.4	7.7	OMEGA [11]
0.5	2.2	2.4	3.2	3.8	5.4	DOLPHIN [12]
0.15	1.2	1.3	1.7	2.1	3.0	GARPUN [13]

2. EXPERIMENTAL SETUP

To achieve the values specified in Table 1, the first stage of a linear HTSC-MAGLEV accelerator is being created at the LPI. This approach is attractive because there is no physical contact between the levitating HTSC-carrier and the accelerator, and as a result, there will be no wear of either component during the CFT delivery especially under high repetition rate operation. Besides, the issue of using the cryogenic lubricants is removed, because their effectiveness at temperatures of T < 20 K is very problematic. Finally, the aim is to avoid additional preheating of the CFT due to mechanical friction, since the permissible variations in the CFT temperature should not exceed 100 mK [14].

The setup includes the following main components: simple and tandem HTSC-carriers and HTSC-MAGLEV accelerator. Three models in the form of a «hollow parallelepiped» (cross section forms a square) were used: model #1: size $25 \times 4 \times 4$ mm, mass 0.97 g; model #2: $37 \times 4 \times 4$ mm, 0.29 g; model #3: $50 \times 4 \times 4$ mm, 0.55 g (Fig. 1). The HTSC-carriers were made from second-generation high-temperature superconductor (2G-HTSC) tapes [15] with a J-PI-04-20Ag-20 Cu structure and a critical superconducting temperature $T_{\rm C} \sim 92$ K. As 2G-HTSC tapes are type II superconductors they allow the magnetic flux lines penetration through their bulk when the applied magnetic field B is between $B_{\rm C1} < B < B_{\rm C2}$, where $B_{\rm C1}$ and $B_{\rm C2}$ are the critical magnetic fields. The penetration of flux lines produces the flux vortices (so-called Abrikosov vortices [16]), the state of which appears as "frozen" in the volume of the superconducting material, and any spatial motion of the superconductor will lead to the motion of the magnetic flux line associated with the vortexes. According to Lenz Law, when an electric current is induced due to a changing magnetic field the direction of the induced current will always oppose the change in the field that caused it. Thus, the effect of the "frozen" flux (flux pinning effect or quantum locking phenomenon) allows fixing the HTSC sample in space, which leads to levitation stability of the acceleration process [16–18].



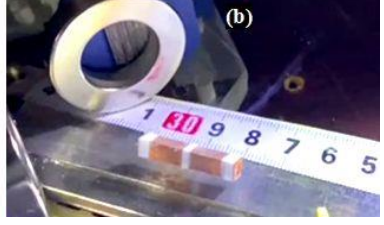


FIG. 1. HTSC-carries used in the experiments. In (a): general view of three carries models at room temperature (T = 300 K); in (b:) HTSC-carrier during levitation (model #1, $T \sim 80$ K).

During levitation, the HTSC-carrier was maintained at a temperature of 80 K $< T_{\rm C} \sim 92$ K at the expense of a polymer foam saturated with liquid nitrogen (T = 77 K) and placed inside it (see Fig. 1a, model #3).

The experiments have confirmed that the 2G-HTSC tapes [15] can be successfully used to maintain a frictionfree motion of the HTSC-carriers, and also to provide a required stability of the levitation height over the whole acceleration length due to the flux pinning effect.

HTSC-MAGLEV accelerator consists of four units (see Fig. 2):

- PMG system with a magnetic track with the following parameters:
 - Size 360x24x5 mm;
- Permanent magnets with an axial magnetization are oriented S-N-S on the track to produce a large cross-sectional gradient [17] (in our case $\Delta B = 0.33$ T):
- Permanent magnets are covered in the middle with an iron collector to guide and concentrate the magnetic flux onto the working magnet surface.
- Such magnetic track architecture is due to the fact that much of the stability during acceleration comes from placing the HTSC-carrier in a magnetic field gradient when there is a strong gradient in one direction and no gradient in the others. For this case, in the PMG construction the magnetic track must allow the HTSCcarriers to move freely only in one direction on account of the existing cross-sectional magnetic-induction gradient according to formula [18]:

$$F = \frac{\chi}{2\mu_s} V_s \frac{dB_y^2}{dy},$$

 $F = \frac{\chi}{2\mu_0} V_s \frac{dB_y^2}{dy},$ where μ_0 is the permeability of vacuum, V_S is the superconductor volume, dB_y^2/dy is the cross-sectional gradient of the magnetic induction. Recall that superconductors are classified as diamagnetic materials with a magnetic susceptibility χ < 0. This allows avoiding any contact of HTSC-carriers with a stronger magnetic field, which pushes out them and return them to their initial trajectory.

- —Trigger system includes a spring mechanism for driving the HTSC-carrier. This is a tightly wound spring about to explode (8-mm-diameter spring and 4-mm-diameter in a compressed state, its height is 15-mm maximum, 4 turns).
- Optical system for tracking HTSC-carrier and injected targets during motion.
- Separation module between HTSC-carrier & target, including a mechanical brake and an injector nozzle.

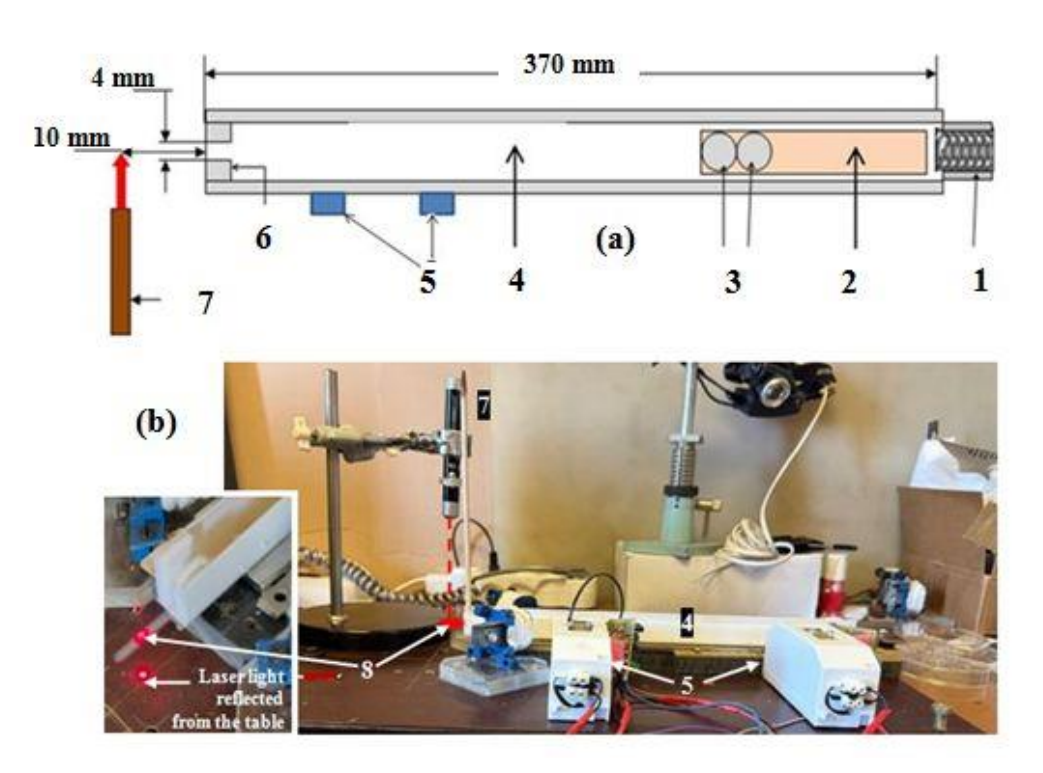


FIG.2 A schematic (a) and a general view (b) of the spring HTSC-MAGLEV accelerator: 1- spring trigger mechanism, 2-HTSC-carrier (T = 80 K), 3 – two surrogate targets (glass beads of 3 mm in diameter), 4 - magnetic track (T = 300 K), 5 – optical sensors for speed measurements of the HTSC-carriers, 6 - mechanical brake and injector nozzle, 7 - laser semiconductor diode ($\lambda = 650$ HM), 8 - injected target.

The processes of both acceleration and deceleration of the levitating HTSC-carrier can be carried out either by mechanical or electromagnetic action [4]. In this work, the carrier driving in the HTSC-MAGLEV system was provided by mechanical action based on a spring mechanism.

A schematic and a general view of the experimental setup are shown in Fig. 2. The magnetic track is a simple combination of neodymium-iron-boron magnets and sheet steels. It consists of 9 rectangular magnets with axial magnetization and residual magnetic induction of 1.45 T. A magnet size is 120 mm \times 8 mm \times 4 mm. The middle three magnets are covered with an iron plate (magnetic flux line collector) having a size of 340 mm \times 10 mm \times 0.5 mm. All construction lies on an iron base with a size of 360 mm \times 24 mm \times 1 mm. The cross-sectional gradient is $\Delta B = 0.33$ T. Directly above the magnetic track, a 24-mm-wide plastic limiter is installed, at the end of which a mechanical brake is mounted with a vertical 3.5-mm-wide nozzle for the flight of the injected target.

The speed of HTSC-carrier was measured according to an optical scheme shown in Fig. 3. After synchronization, each radiation detector located at a certain distance L from each other records the moments of intersection of the HTSC-carrier with a laser beam: t_1 and t_2 . Hence, the HTSC-carrier speed can be simply defined as $v = L/\Delta t$. The accuracy of determining the coordinates is ± 1 mm at a base distance L = 200 mm. The accuracy of determining the radiation detector response is ± 20 μ s. The speed measurements of the HTSC-carriers of various geometry in the spring HTSC-MAGLEV accelerator showed the values in the range of 2.8-7.1 m/s.

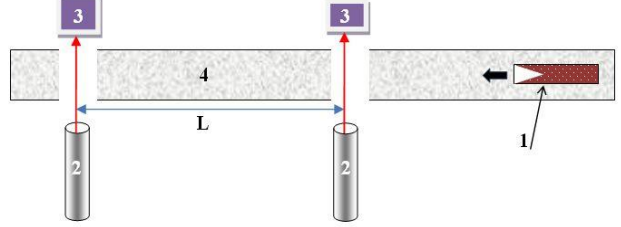


FIG.3 Optical scheme for speed measurements of the HTSC-carriers: 1 – HTSC-carrier, 2 – He-Ne continuous-wave laser, 3 – laser radiation detector, 4 – magnetic track.

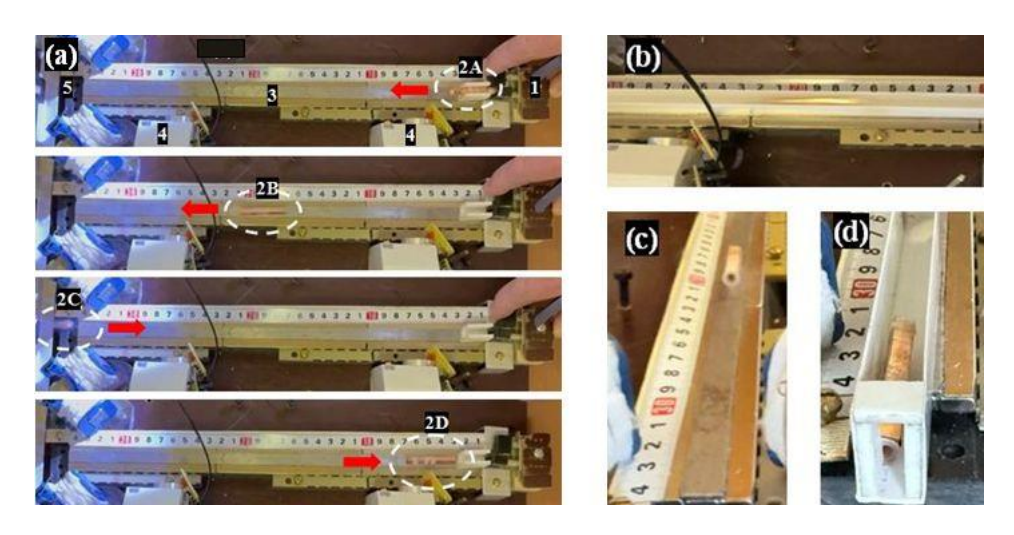


FIG. 4. Testing of the magnetic track alignment. In (a): 1 – spring trigger mechanism, 2 – HTSC-carrier (A – HTSC-carrier at the start of its guide lane, B – HTSC-carrier in the middle of the magnetic track, C – HTSC-carrier reflection at the magnetic track end, D – return of the HTSC-carrier at the starting position), 3 – magnetic track, 4 – HTSC-carrier speed sensors, 5 – mechanical brake. In (b): HTSC-carrier levitation at $v \sim 7$ m/c (model #2); in (c): HTSC-carrier with a target nest from a full density polymer levitates at $v \sim 3$ m/c (model #3); in (c): HTSC-carrier in front of the nozzle after the target injection.

Alignment of the magnetic track was tested experimentally according to Fig. 4. The cartridge (1) of the trigger mechanism contains the HTSC-carrier (pos. 2A) which is fired for its placement over the magnetic track (3). The HTSC-carrier begins to levitate along the magnetic track (pos. 2B) to the end point (5), in which it is reflected (pos. 2C) and then it returns to the beginning of the path (pos. 2D). Thus, we have a levitating HTSC-carrier, which is free to move back and forth exactly along the magnetic track. In this case, namely the magnetic gradient $\Delta B = 0.33$ T limits its deviations in the transverse direction from the given trajectory.

3. RESULTS AND DISCUSSION

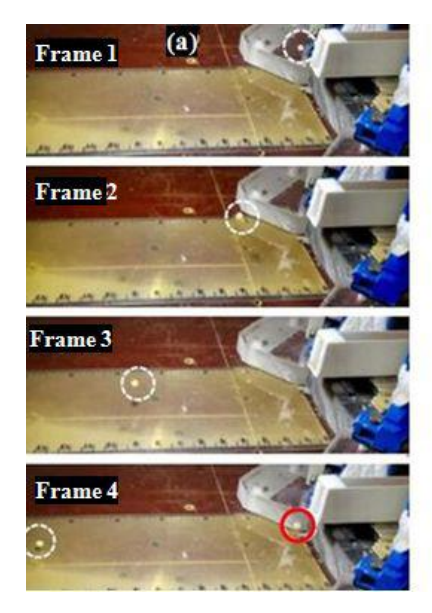
The following results were obtained in the experiments:

- The HTSC-carrier like tandem was used (two surrogate targets inside one carrier).
- The speed of the HTSC-carrier for one stage of the MAGLEV accelerator was in the range of 1.2–7.1 m/s, what is fallen within the range of Table 1. The low speeds correspond to a manual start-up of HTSC-carrier motion
- The gap between the HTSC-carrier and a magnetic rail was no varying with time, i.e. the levitation drift during the HTSC-carrier motion is absent.
- The injection rate was in the range of 10–25 Hz. It depends on the material from which the target nest inside HTSC-carrier is made.
- The acceleration of the HTSC-carrier with a subsequent braking and then an injection of two surrogate targets (glass beads) were recorded (Fig. 5 and 6). The time interval between the injection of two targets was \sim 0.1 s (Fig. 5, target nest inside HTSC-carrier is from a foam polymer) and 0.04 s (Fig. 5, target nest from a full density polymer), which corresponds to an injection rate of \sim 10 Hz and \sim 25 Hz, correspondingly.
- In the experiments, a hard braking was carried out mechanically, but the possibilities of soft electromagnetic influence on the deceleration process were discussed (Fig. 7 and 8).
- These results are the bases for high-repetition injection of solid spherical polymer beads (polystyrene, deuterated polystyrene and some others) with different diameters.

Fig. 5 demonstrates stop-frames of the video recording of two targets injection one after another obtained in continuous light of semiconductor LD. The target nest is made from a foam polymer. The time interval between the injection of two targets is ~0.1 s, and the injection rate is 10 Hz.



Fig.5 Two targets injection at a rate of 10 Hz using a tandem HTSC-carrier (model #3): frame 1 – before injection; frame 2 – the 1st injected target crosses the laser light; frame 3 – the point of 2nd target injection; frame 4 – the 2nd injected target crosses the laser light.



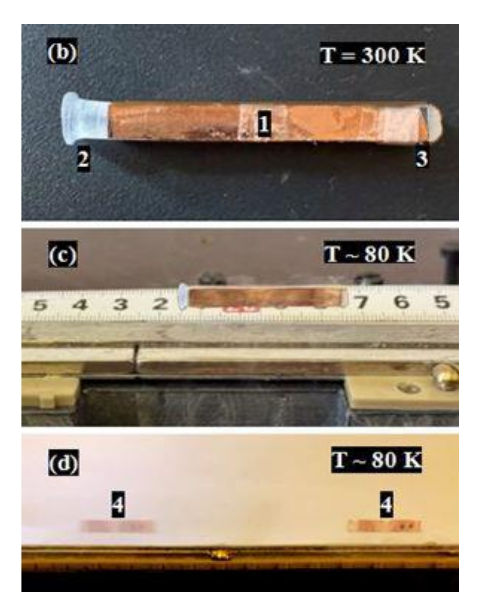


FIG.6 Two targets injection at a rate of 25 Hz using a tandem HTSC-carrier (model #3). In (a): frame 1 – the point of 1^{st} target injection (shown in white dotted line), frames 2 and 3 – 1^{st} target in flight, frame 4 – the point of the 2^{nd} target injection (shown in red solid line); in (b): general view of the tandem HTSC-carrier (1 – HTSC-carrier housing; 2 – target nest from a full density polymer, 3 – polymer foam for saturating with liquid nitrogen); in (c): tandem HTSC-carrier levitation; in (d) sequential launch of two HTSC-carriers into the MAGLEV accelerator (4 – HTSC-carrier for a single target, model #1).

IAEA-CN-316/INDICO ID #2680

Fig. 6 demonstrates stop-frames of the video recording of two targets injection one after another obtained in the strobe system. The target nest is made from a full density polymer. Time interval between the injection of two targets is ~0.04 s, and the injection rate is 25 Hz. Fig. 6d shows a sequential launch of two HTSC-carriers into the MAGLEV accelerator that shows another scenario for target delivery by injection.

Ending this section note that a hard braking after a powerful acceleration, which will be essential attributes of the CFT delivery, can be a big problem for IFE reactor, which is as follows: a fragile CFT must survive deceleration process without damage. Therefore, for a nearest future a step-change in deceleration technology will be required to meet the 10-Hz requirements for reactor-scaled CFTs. We have started with a soft electromagnetic option of the carrier deceleration and performed the proof-of-principle experiments.

Since the braking process is a part of separation process between the HTSC-carrier and the target, we will consider just the electromagnetic option when the properties of HTSC materials can be used optimally for both separation and braking operation. In the process of separation which can be done with a set of permanent magnets or field coils, the HTSC-carrier drops its velocity during its motion in the growing magnetic field according to formula (1), while the target keeps its velocity moving forward by inertia (target is nonmagnetic and it is not affected by the magnetic field).

In this regard, we made changes in the design of the separation module. The principal of its operation is shown in Fig. 7. To influence the HTSC-carrier, two ring permanent magnets based on neodymium-iron-boron (NdFeB) with an anti-corrosion coating of Ni-Cu-Ni (Nickel) were used. The magnet dimensions are: outer diameter -35 mm, inner diameter -20 mm, height -8 mm. A residual magnetic induction B=1.4 T. The HTSC-carrier is thrown vertically from a height of 10 cm with a zero initial velocity (on the ground its speed is 1.4 m/s). During free fall it enters the increasing magnetic field. As the HTSCs are diamagnetic, the HTSC-carrier is pushed out from the area of a stronger magnetic field.

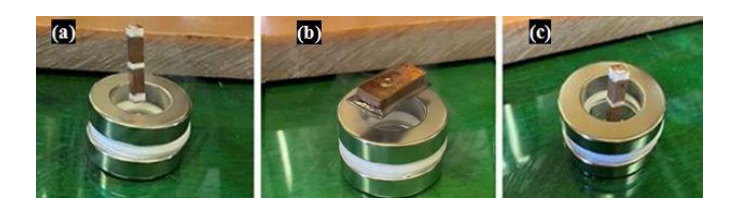


FIG.7 Vertical deceleration of the HTSC-carrier of a «hollow parallelepiped» type with a polymer foam saturated with liquid nitrogen in a gradient magnetic field.

Under these conditions the carrier stops and becomes suspended over a magnet at a certain height (Fig. 7a). This height does not change unless HTSC-carrier temperature changes. Its value depends on the time before the HTSC warms from $T \sim 80$ K back up to the transition temperature $T_{\rm C} \sim 92$ K. To avoid rapid heating different insulation materials were used in the experiments. For models in the form of a «hollow parallelepiped» it is a polymer foam saturated with liquid nitrogen (Figs.7a and 7c). For models in the form of «open parallelepiped» (length inside 25 mm, width inside 8 mm, height 4 mm, total mass 1.25 g, see Fig.7b) it is a liquid nitrogen (boiling point 77 K) was poured directly into the HTSC-carrier (Fig. 7b). Obviously, the case shown in Fig.7b is preferable – the height does not change for a long time until the liquid helium boils away. To achieve such results for the «hollow parallelepiped» carriers, it is planned to use new HTSC materials with porosity above 50%. The pores in such HTSCs provide a better penetration of a coolant, efficient heat removal and stable operation [19].

Below we present a proof-of-principle demonstration of the method of braking the HTSC-carrier to separate a target with the same permanent magnets as in Fig. 7. To manipulate the rate of horizontal braking one must adjust either the magnitude or duration of magnetic force (braking impulse) applied in the horizontal direction to provide stable and smooth movements of the HTSC-carrier in the MAGLEV accelerator (Fig. 8). Inour case, the magnets were located at an angle or parallel each other. The speed of the HTSC-carrier was 1.2 m/c (Fig. 8a,b, d) and 3.2 m/c (Fig. c, f). Note that in the process of magnetic braking, three main parameters play a role: temperature, HTSC-carrier speed and magnetic force field ($B_r \times dB_r/dr$, where r is a coordinate directed along the acceleration length). Since in our experiments (Fig. 8) the braking time was several seconds, the influence of temperature can be excluded.

The results of demonstrating the magnetic braking impulse are as follows: 1) if the HTSC-carrier speed is less than 1.5 m/c, then the carrier braking is successful; 2) otherwise the HTSC-carrier flies through the magnetic field without braking regardless of how the magnets are located.

Fig. 7c shows how to change the HTSC-carriers orientation to remove them from the MAGLEV accelerator after target injection. This is an important step in the development of HTSC-carrier separation module whose operation is based on using a special coil with a pulsed, repetitively cycled signal to direct the used HTSC-carriers into a special collection system.

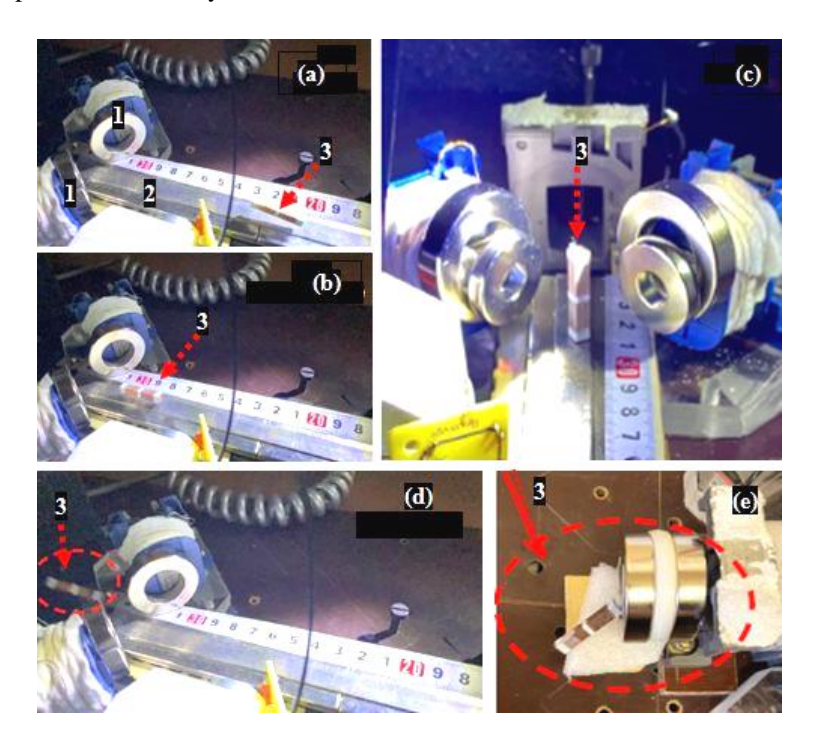


FIG.7. Proof-of-principle experiments: HTSC-carrier braking using magnets located at an angle (a-d) or parallel (f) each other (1-magnets, 2-magnetic track, 3-HTSC-carrier). In (a): HTSC-carrier during motion at 1.2 m/c; in (b): HTSC-carrier during successful braking; in (c): changing the direction of the magnetic field allows the HTSC-carrier to be turned by 90° ; in (d): HTSC-carrier during motion at 3.2 m/c without braking by magnets located at an angle each other; in (e): HTSC-carrier at 3.2 m/c freely passes through the entire braking zone at parallel magnets location as well.

Thus, to manipulate the HTSC-carrier braking or its orientation for removing from acceleration system it is necessary to create the required magnetic field gradient for a given HTSC-carrier speed. For existing laser facilities these values are not high ($v_{\rm inj} = 3.2-17$ m/s; $T_{\rm ch} = 300$ K and $R_{\rm ch} = 1-5$ m [6]). But for the IFE reactor ($v_{\rm inj} = 200-400$ m/s; $T_{\rm ch} \sim 1758$ K and $R_{\rm ch} \sim 6$ m) [5]) it is important to highlight that the optimization of braking impulse will require a high level of technical ability.

4. CONCLUSION

A step-change in CFT injection technology is required to meet the ICF/IFE requirements for high repetition rate (HRR) conditions. This is now being realized at the LPI in the development of HTSC-MAGLEV technologies for injection delivery of CFTs at the laser focus both in a single and repeatable mode. Our approach is based on the phenomenon of quantum levitation of a superconducting target carrier (HTSC-carrier) in gradient magnetic fields. To meet these challenging HRR-requirements, a setup for demonstrating the injection capabilities was build using spring launch technology combined with magnetic levitation, allowing no heat energy transfer into the CFT from the accelerating medium. And in doing so, a CFT overheating will be excluded in terms of loss of quality of the D-T layers, and a service life of the delivery system will be extended, especially when it operates under HRR conditions. Experiments and modeling have confirmed the prospects of this approach [20]. In this work, we used the created setup with the magnetic track having a cross-sectional induction gradient $\Delta B = 0.33$ T to provide a required stability of the levitation height over the whole acceleration length. A series of injection tests were conducted to verify a tandem HTSC-carrier configuration. The motion of the tandem HTSC-carrier containing two surrogate targets was recorded, followed by its mechanical braking and targets injection with a rate of 10 Hz (target nest from a foam polymer) and 25 Hz (target nest from a full density polymer). Because in IFE experiments a fragile CFT must survive the braking process without damage, the potentials of a soft

IAEA-CN-316/INDICO ID #2680

electromagnetic braking were also analyzed. Proof-of-principle experiments have shown the possibility to manipulate both the magnetic braking of the HTSC-carrier and its orientation after separation between the target and HTSC-carrier. The latter is a necessary element when creating the HTSC-carrier separation module to remove the used carriers from the HTSC-MAGLEV accelerator. Further developments of this direction will allow planning unique experiments on a uniform, spherically symmetric laser irradiation of CFTs injected into the reaction chamber of existing laser facilities capable of ignition-level performance.

ACKNOWLEDGEMENTS

This work was performed within the framework of the State Assignment of the LPI

REFERENCES

- [1] ALEKSANDROVA, I.V. AND KORESHEVA, E.R., Review on high repetition rate and mass production of the cryogenic targets for laser IFE. High Power Laser Sci. Eng. 5 2 (2017) e11 (21 pp).
- [2] KRITCHER, A.L., SCHLOSSBERG, D. J., WEBER, C. R., et al. Design of first experiment to achieve fusion target gain > 1. Phys. Plasmas **31** (2024) 070502.
- [3] ALEKSANDROVA, I.V., KORESHEVA, E.R., KOSHELEV, E.L. Target fabrication technologies and noncontact delivery systems to develop a free-standing target factory operating in the repetition mode at the IFE relevant level. Nuclear Fusion 61 12 (2021) 126009 (7 pp).
- [4] ALEKSANDROVA, I.V., KORESHEVA, E.R., AND KOSHELEV, E.L., A High-Pinning-Type-II Superconducting Maglev for ICF Target Delivery: main principles, material options and demonstration models. High Power Laser Sci. Eng. 10 (2022) e11 (15 pp).
- [5] GOODIN, D.T., ALEXANDER, N.B., BROWN, L.C., et al. A cost-effective target supply for inertial fusion energy. Nuclear Fusion 44 12 (2004) S254–265.
- [6] ALEKSANDROVA, I. V., AKUNETS, A. A., AGAPOV, M. N., KORESHEVA, E. R., NIKITENKO, A. I. Injection delivery of cryogenic fuel targets using levitation into the laser focus of operating ICF facilities. Quantum Electronics 55 2 (2025) 102-120 (in Russian)
- [7] BRANDON, V., CANAUD, B., TEMPORAL, M., RAMIS, R. Low initial aspect-ratio direct-drive target designs for shock- or self-ignition in the context of the laser Megajoule. Nuclear Fusion **54** 8 (2014) 083016 (12 pp)
- [8] BEL'KOV, C. A., GARANIN, S. G., SHAGALKIN, YU. V. Installation of UFL-2M, the first steps towards its creation. Report, XL International conf. on Plasma Physics & Controlled Fusion, Zvenigorod (Moscow sub.), Russian Federation February 11-15, 2013.
- [9] KRAMER, D. NIF success gives laser fusion energy a shot in the arm. Physics Today 76 3 (2023) 25-27.
- [10] MIQUEL, J-L., BATANI, D., BLANCHOT, N. Overview of the laser mega joule (LMJ) facility and petal project in France. The review of laser engineering 42 2 (2020) 131-136.
- [11] Omega Target Chamber. https://www.flickr.com/photos/departmentofenergy/16448799001/in/photostream/
- [12] BASOV, N. G., ALLIN, A. P., BYKOVSKIY, N. E., et al. Laser thermonuclear installation "Dolphin": the operating complex and directions of development. Trudy FIAN 178 (1987) 3-88. (in Russian)
- [13] ZVORYKIN, V.D., DIDENKO, N.V., IONIN, A.A., et al. GARPUN-MTW: A hybrid Ti: Sapphire/KrF laser facility for simultaneous amplification of subpicosecond/nanosecond pulses relevant to fast-ignition ICF concept. Laser and Particle Beams 25 3 (2007) 435-451.
- [14] MILES R., SPAETH M., MANES K., et al. Challenges surrounding the injection and arrival of targets at life fusion chamber center. Fusion Sci. Technol. **60** 1 (2011) 61-65.
- [15] LEE, S., PETRYKIN, V., MOLODYK, A., et al. Development and production of second generation high Tc superconducting tapes at SuperOx and first tests of model cables. Superconductors Science and Technology 27 4 (2014) 044022 (9 pp)
- [16] ABRIKOSOV, A. A. On the Magnetic properties of superconductors of the second group. J. Exp. Theor. Phys. 32 (1957) 1442-1452
- [17] GINZBURG, V. L., ANDRYUSHIN, E. A. Superconductivity. Revised Edition. World Scientific, Singapore (2006).
- [18] LANDAU, L. D., LIFSHITZ, E. M. Theoretical Physics. Electrodynamics of Continuous Media, 2-nd Edition. NAUKA, Moscow (1982).
- [19] GOKHFELD, D., KOBLISHKA, M., KOBLISHKA-VENEV, A. HIGHLY POROUS SUPERCONDUCTORS: SYNTHESIS, RESEARCH, AND PROSPECTS. Phys. METALS AND METALLOGRAPHY 121 10 (2020) 936-948.
- [20] ALEKSANDROVA, I. V., KORESHEVA, E. R., AKUNETS, A. A., et al. Cryogenic target delivery for laser IFE status and future challenges. Bull. Lebedev Phys. Inst. **51** 6 (2024) S472-S488.